Photocatalytic reaction on photofuel cell titania electrode

Hiromasa Nishikiori,* Yotaro Kato, and Tsuneo Fujii

Department of Environmental Science and Technology, Faculty of Engineering, Shinshu University, 4-17-1 Wakasato, Nagano 380-8553, Japan

Corresponding author: Hiromasa Nishikiori

Tel: +81-26-269-5536

Fax: +81-26-269-5550

E-mail: nishiki@shinshu-u.ac.jp

Department of Environmental Science and Technology, Faculty of Engineering, Shinshu University, 4-17-1 Wakasato, Nagano 380-8553, Japan

Abstract

Benzoic acid-doped titania electrodes were prepared from titanium alkoxide sols containing benzoic acid in order to examine the photocatalytic reaction of the fuel material concentrated on the titania surface of a photofuel cell electrode. This doping was developed in order to understand the physicochemical processes on the titania rather than to advance the practical use of the photofuel cells. The observed photocurrent and CO_2 and H_2O productions indicated that the oxidation of the benzoic acid enhanced the generation of electricity during the UV irradiation. Benzoic acid molecules should be oxidized by oxygen molecules and holes on the titania surface. The steam treatment of the electrodes improved the benzoic acid oxidation and the photocurrent because it promoted the titania densification and enhanced the interaction between the benzoic acid and titania. The benzoic acid-doped titania is a valid model of the fuel material concentrated in the porous titania when using benzoic acid as the fuel material. The contact between the benzoic acid and titania is important in order to obtain a high photofuel electric conversion.

Keywords: Photofuel cell; Titania; Photocatalysis; Benzoic acid; Oxidation

Introduction

Photocatalyst titania films are useful as photofuel cell electrodes to generate electricity by oxidizing the fuel materials during UV irradiation [1−6]. Photofuel cells are expected to allow both the disposal of organic wastes and electric generation. The photofuel working electrodes generally act in the liquid phase containing the fuel material. In such systems, the concentration of the fuel material on the photocatalyst surface is one of the parameters that can improve the energy conversion efficiency. The contact between the fuel material and titania is also important for the effective generation.

Dye-adsorbed titania films are used as the working electrodes of dye-sensitized solar cells [7−9]. In such systems, the electron injection from the dye to the titania is important. We previously investigated dye-doped amorphous titania gels prepared without heating from a titanium alkoxide sol containing the dye molecules [10−14]. The characteristics of the dye-doped titania system include a high dispersion of the dye and a high contact area between the dye and titania. The dye-doped titania system is an interesting material for the basic study of dye-sensitized solar cells because hydrothermal treatments cause its crystallization and changes in the titania structure and dye-titania bond character. The dye-doped titania electrodes were prepared from an untreated or refluxed [13,15−19] titanium alkoxide solution containing the dye. These electrodes were then treated with steam in a sealed container [20−23]. The amorphous titania was changed into nanocrystalline anatase by hydrothermal treatment at a low temperature. We then studied the photoelectric conversion properties of the dye-doped nanocrystalline titania films. The conversion efficiency was improved by enhancing the dye−titania interaction due to the hydrothermal treatments [10−14].

In this study, the benzoic acid-doped titania electrodes were prepared by the steam treatment of the gel film produced from the precursor sol containing benzoic acid. We

investigated the photocatalytic reaction of benzoic acid as a fuel material on the titania surface of the fuel cell electrode. The fuel material doping is one of the methods to immobilize a certain amount of it on the titania. The benzoic acid-doped titania is a model of the fuel material concentrated in the porous titania. This doping was developed in order to understand the physicochemical processes on the titania rather than to advance the practical use of the photofuel cells. This study was conducted in order to examine the interaction between the benzoic acid and titania, the photocatalytic reaction of benzoic acid on the titania, and their influence on the photofuel cell performance.

Experimental

Materials

Titanium tetraisopropoxide (TTIP), nitric acid (69−70%), ethanol, benzoic acid, iodine, and lithium iodide of S or reagent grade were obtained from Wako Pure Chemicals. The dry nitrogen gas was obtained from Okaya Sanso. These materials were used without further purification. The water was deionized and distilled (Yamato WG23).

Sample preparation

The sol-gel reaction system was prepared by mixing 5.0 cm^3 of TTIP, 25.0 cm^3 of ethanol, 0.21 cm^3 of water, and 0.21 cm^3 of nitric acid as the catalyst for the sol-gel reaction and labeled SG. The mixing was carried out in a nitrogen atmosphere. Benzoic acid was dissolved in the SG to a final concentration of 1.1×10^{-2} mol dm^{-3} and this system was labeled SG-BA. The dip-coated thin films were made from the systems in which the sol-gel reaction occurred for 1 day to prepare the electrodes.

In order to prepare the electrode samples coated with the crystalline titania, the glass plates with the ITO transparent electrode were dip-coated with the SG and then heated at 500

ºC for 30 min. These electrodes were labeled E0. Furthermore, the working electrodes were prepared in which the E0 was dip-coated with the SG-BA and SG. These electrodes were labeled WE-N-BA and WE-N, respectively.

Water was heated at 100 ºC and then these electrode samples were exposed to its steam for 2 h. The steam pressure was about 100 kPa [10−14]. The steam-treated working electrodes prepared from the SG-BA and SG were labeled WE-N-s-BA and WE-N-s, respectively.

The titania films, F-N and F-N-s, and the benzoic acid-doped titania films, F-N-BA and F-N-s-BA, were also prepared on glass plates without ITO for the XRD analyses.

Characterization of samples

The prepared samples were characterized by SEM observations (Hitachi S-4100) and XRD analysis using CuKα radiation (Rigaku RINT-2000V). The layer thickness of the electrode samples was estimated from their cross section by SEM observation. The size of the crystallites of each sample was estimated from its full-width at half-maximum of the 25.3° peak in the XRD pattern using Sherrer's equation, $D=0.9\lambda/\beta\cdot\cos\theta$.

The iodine-based electrolyte (I_2/LiI) was allowed to soak into the space between the working electrode sample and the counter Pt electrode. The $I-V$ curves of the electrodes were measured during irradiation by a 150 W Xe short arc lamp (Hokuto Denko HSV-100). In this study, a nonaqueous iodine-based electrolyte was used for the electrochemical measurement in order to induce the oxidation and reduction on/near the titania surface without producing hydrogen or the superoxide anion radical on the counter electrode.

The concentrations of CO_2 and H_2O produced during the photocatalytic degradation in an IR spectroscopic cell (100 cm^3) were estimated by an FTIR analysis (Shimadzu IRPrestige-21) [24−27]. The flakes of the film samples were pressed in KBr pellets and

their FTIR spectra were taken in order to examine the photocatalytic degradation of the doped benzoic acid.

Results and discussion

Characterization of the samples

Figure 1 shows the SEM images of the steam-treated titania electrodes with and without benzoic acid, WE-N-s-BA and WE-N-s, respectively. No particles were observed in the untreated electrodes, WE-N-BA and WE-N, and they appeared amorphous (data not shown). Both electrodes mainly consisted of ca. 10−20 nm particles. The benzoic acid doping slightly influenced the particle growth of the titania. The thickness of the unheated electrode titania layer was 120−150 nm and slightly changed after the steam treatment.

(Figure 1)

Figure 2 shows the XRD patterns of the titania films, F-N and F-N-s, and the benzoic acid-doped titania films, F-N-BA and F-N-s-BA. The untreated films, F-N and F-N-BA, exhibited no diffraction peaks and were found to be amorphous. The 2θ peak at around 25° was observed in the XRD patterns of the steam-treated films, F-N-s and F-N-s-BA, indicating that an anatase-type crystal was produced by the steam treatment of the gels. However, the peak intensity was weaker for the benzoic acid-containing film, F-N-s-BA, than for the benzoic acid-free film, F-N-s. Although the crystallite size of F-N-s was estimated to be 2.3 nm using Sherrer's equation, that of F-N-s-BA was too small to be calculated. These results indicated that benzoic acid molecules prevented the crystal growth of the titania [11]. In some cases, the titania crystallization process influenced the benzoic acid dispersion as reported for the dye-doped systems [13]. However, the benzoic acid molecules should be highly dispersed in the present sol. The organic molecules were doped and dispersed into

the titania on a molecular level during the sol-gel process [28−31]. Therefore, the molecular aggregates cannot expand the pore size of the titania. The pore size or porosity does not depend on the presence of the benzoic acid molecules.

(Figure 2)

Photofuel electric conversion

Figure 3 shows the *I*−*V* curves of the titania electrodes, WE-N and WE-N-s, and the benzoic acid-doped titania electrodes, WE-N-BA and WE-N-s-BA, during light irradiation. The photoelectric conversion properties are summarized in Table 1. The dark reaction was negligible in this study because the current density was observed to be lower than 1 μA cm^{-2} in the dark. The *I*−*V* curve shapes and the short circuit photocurrent and open circuit voltage values of the untreated titania electrodes slightly depended on the presence of the benzoic acid. The untreated electrode did not undergo photocatalytic degradation or photoelectric enhancement. On the other hand, higher short circuit photocurrent values were clearly observed for the steam-treated benzoic acid-doped electrode than for the normal titania electrode. Their short circuit photocurrent and open circuit voltage values were higher than those of the untreated electrodes. The steam treatment definitely improved the photocurrent and photofuel cell reaction even though it did not significantly improve the crystallinity of the titania. As previously reported, hot water molecules promoted the polymerization of the alkoxide species and the network growth of the metal oxide [10−14]. These results indicated that the conversion efficiency was improved by enhancement of the electric conductivity due to slight densification and crystallization of the titania. The steam treatment of the electrode was effective for the photofuel cell reaction, i.e., the interaction between the fuel material and titania due to the titania densification.

(Figure 3 and Table 1)

With respect to the interaction, the concentration of the fuel material on the photocatalyst

surface is an important parameter to improve the energy conversion efficiency. The benzoic acid molecules should be oxidized with oxygen molecules and holes on the titania surface and produce protons. The protons and oxygen molecules should be reduced by electrons due to the electrolyte as follows:

$C_6H_5COOH + h^+ \rightarrow C_6H_5\cdot + CO_2 + H^+$

$C_6H_5\cdot + 6O_2 + 5h^+ \rightarrow 6CO_2 + 5H^+$

$6H^+ + 3/2O_2 + 6e^- \rightarrow 3H_2O$

Oxidation of benzoic acid

CO_2 and H_2O were observed as the photocatalytic products from the benzoic acid-doped titania electrodes during light irradiation. Figure 4 shows the time course of the concentrations of CO_2 and H_2O produced during the photocatalytic degradation of benzoic acid for each benzoic acid-doped titania electrode. The initial production rates of CO_2 and H_2O, i.e., the average rates for the initial 60 min, were estimated to be 2.0×10^{-8} and 6.8×10^{-9} mol min^{-1}, respectively. Their concentrations increased with the irradiation time and approached saturation after a 3-h irradiation. The CO_2 concentration after the 3-h irradiation is about twice that of H_2O, indicating that the benzoic acid molecules are completely oxidized on the titania surface. The amount of the benzoic acid degraded during the 3-h UV irradiation was 2.2×10^{-8} mol, which corresponded to more than 90% of the doped benzoic acid.

(Figure 4)

Figure 5 shows the FTIR spectra of the steam-treated benzoic acid-doped titania electrode, WE-N-BA, before and after the UV irradiation. The spectrum before the UV irradiation exhibited peaks at 1520 and 1420 cm^{-1} for the carboxylate COO^- antisymmetric and symmetric stretching vibrations, respectively, at 1600 cm^{-1} for the skeleton vibration of the benzene ring, and at 1120, 1080, and 1020 cm^{-1} for the C−H in-plane bending vibration of the

benzene ring. In addition, this spectrum has a peak at 1620 cm^{-1} assigned to the O−H bending vibration of the adsorbed water, a peak at 1380 cm^{-1} for the N−O stretching vibration of NO_3^-, and a peak at 1000−600 cm^{-1} assigned to the Ti−O stretching vibration of the titania. The bands assigned to benzoic acid almost disappeared after the 3-h UV irradiation due to its photocatalytic degradation. The carboxyl group of benzoic acid was transformed into the carboxylate and formed a chelate complex with the titanium species as reported in the fluorescein-doped titania [14]. This is because the proton dissociation constant, pK_a, of the carboxyl group of benzoic acid, i.e., 4.2, is close to that of fluorescein, i.e., 4.45 [32]. The FTIR spectrum suggests that a dehydration between the carboxyl group of benzoic acid and the OH group on the titania surface induced the chelating linkage.

(Figure 5)

The increase in the photocurrent density due to the photocatalytic degradation of benzoic acid was estimated to be 4.2 μA cm^{-2} from the average production rate of CO_2 during the initial 60 min. The increase in the short circuit photocurrent density due to the benzoic acid doping was estimated to be 2.9 μA cm^{-2} from the *I*−*V* curves in Figure 3. The current generation efficiency, i.e., the ratio of the photocurrent to the CO_2 production rate due to the benzoic acid degradation, is 69%. In the benzoic acid-doped titania electrode, the photocurrent and CO_2 and H_2O productions were observed even though the titania crystallinity was low. This is not due to the significant contribution of the titania crystallinity to the photocurrent generation. It is important for the photofuel reaction that the benzoic acid molecules were highly dispersed and incorporated in the titania. As shown in Figure 5, the carboxylate bands of the doped benzoic acid indicate the strong interaction and a chelating linkage between the carboxylate and the titanium species [14]. In systems, such as dye-sensitized titania solar cells, the strong interaction and complex formation between the organic molecules and titania caused the ligand-to-metal charge

transfer (LMCT) interaction and a fast electron injection into the titania conduction band [33−35]. The reactivity was influenced by the contact between the benzoic acid and titania [13,14]. The chelating linkage between the benzoic acid and the titania promoted the oxidation of the benzoic acid and the CO_2 production during the UV irradiation due to efficient hole transfer.

Conclusions

The benzoic acid-doped titania electrodes were prepared from titanium alkoxide sols containing benzoic acid, followed by steam treatment, and their photoelectric properties were investigated in order to examine the interaction between the benzoic acid and titania. The higher photocurrent values were clearly observed for the benzoic acid-doped electrode than for the normal titania electrode. This indicates that the oxidation of the benzoic acid enhanced the generation of electricity. CO_2 and H_2O were observed as the photocatalytic products from the benzoic acid-doped titania electrodes during the UV irradiation. The benzoic acid molecules should be oxidized by oxygen molecules and holes on the titania surface and produce protons. The protons and oxygen molecules should be reduced by electrons due to the electrolyte. The steam treatment of the electrodes improved the benzoic acid oxidation and the photocurrent. Not only the titania conductivity due to its crystallinity, but also the contact between the fuel material and titania due to its dispersion in the titania are important for a high photofuel electric conversion. The steam treatment promoted the titania densification and improved the interaction between the benzoic acid and titania. The benzoic acid-doped titania is a valid model of the fuel material concentrated in the porous titania when using benzoic acid as the fuel material. The interaction between the fuel material and the photocatalyst surface is an important parameter to improve the energy conversion efficiency.

References

[1] M. Kaneko, J. Nemoto, H. Ueno, N. Gokan, K. Ohnuki, M. Horikawa, R. Saito, T. Shibata, Electrochem. Commun. 8, 336 (2006)

[2] H. Ueno, J. Nemoto, K. Ohnuki, M. Horikawa, M. Hoshino, M. Kaneko, J. Appl. Electrochem. 39, 1897 (2009)

[3] M. Antoniadou, P. Lianos, Catal. Today 144, 166 (2009)

[4] M. Antoniadou, D. I. Kondarides, D. Labou, Catal. Lett. 129, 344 (2009)

[5] M. Antoniadou, P. Lianos, Appl. Catal. B-Environ. 99, 307 (2010)

[6] M. Antoniadou, D. I. Kondarides, D. Labou, S. Neophytides, P. Lianos, Sol. Energy Mater. Sol. cells 94, 592 (2010)

[7] B. O'Regan, M. Grätzel, Nature 353, 737 (1991)

[8] M. K. Nazeeruddin, A. Kay, I. Rodicio, R. Hamphry-Baker, E. Müeller, P. Liska, N. Vlachopoulos, M. Grätzel, J. Am. Chem. Soc. 115, 6382 (1993)

[9] M. Grätzel, J. Photochem. Photobiol. C-Photochem. Rev. 4, 145 (2003)

[10] H. Nishikiori, N. Tanaka, T. Kitsui, T. Fujii, J. Photochem. Photobiol. A-Chem. 179, 125 (2006)

[11] T. Kitsui, H. Nishikiori, N. Tanaka, T. Fujii, J. Photochem. Photobiol. A-Chem. 192, 220 (2007)

[12] H. Nishikiori, W. Qian, M. A. El-Sayed, N. Tanaka, T. Fujii, J. Phys. Chem. C 111, 9008 (2007)

[13] H. Nishikiori, Y. Uesugi, N. Tanaka, T. Fujii, J. Photochem. Photobiol. A-Chem. 207, 204 (2009)

[14] H. Nishikiori, Y. Uesugi, S. Takami, R. A. Setiawan, T. Fujii, W. Qian, M. A. El-Sayed, J. Phys. Chem. C 115, 2880 (2011)

[15] Y. Hu, C. Yuan, J. Cryst. Growth 274, 563 (2005)

[16] L. Ge, M. Xu, M. Sun, H. Fang, J. Sol-Gel Sci. Technol. 38, 47 (2006)

[17] S. Liu, N. Jaffrezic, C. Guillard, Appl. Surface Sci. 255, 2704 (2008)

[18] S. Zhang, Z. Chen, Y. Li, Q. Wang, L. Wan, Y. You, Mater. Chem. Phys. 107, 1 (2008)

[19] S. Priya, J. Robichaud, M. C. Méthot, S. Balaji, J. M. Ehrman, B. L. Su, Y. Djaoued, J. Mater. Sci. 44, 6470 (2009)

[20] K. Yanagisawa, J. Ovenstone, J. Phys. Chem. B 103, 7781 (1999)

[21] K. Y. Chiu, M. H. Wong, F. T. Cheng, H. C. Man, Appl. Surf. Sci. 253, 6762 (2007)

[22] D. P. Serrano, G. Calleja, R. Sanz, P. Pizarro, J. Mater. Chem. 17, 1178 (2007)

[23] M. H. Wong, F. T. Cheng, H. C. Man, J. Am. Ceram. Soc. 91, 414 (2008)

[24] R. J. Haines, R. E. Wittrig, C. P. Kubiak, Inorg. Chem. 33, 4723 (1994)

[25] R. A. Nicodemus, A. Tokmakoff, Chem. Phys. Lett. 449, 130 (2007)

[26] H. Nishikiori, M. Tagahara, L. Mukoyama, T. Fujii, Res. Chem. Intermed. 36, 947 (2010)

[27] H. Nishikiori, M. Furukawa, T. Fujii, Appl. Catal. B-Environ. 102, 470 (2011)

[28] T. Fujii, H. Nishikiori, T. Tamura, Chem. Phys. Lett. 233, 424 (1995)

[29] H. Nishikiori, T. Fujii, J. Phys. Chem. B 101, 3680 (1997)

[30] H. Nishikiori, S. Nagaya, N. Tanaka, A. Katsuki, T. Fujii, Bull. Chem. Soc. Jpn. 72, 915 (1999)

[31] H. Nishikiori, N. Tanaka, Y. Minami, A. Katsuki, T. Fujii, J. Photochem. Photobiol. A-Chem. 212, 62 (2010)

[32] N. O. Mchedlov-Petrossyan, V. N. Kleshchevnikova, J. Chem. Soc., Faraday Trans. 90, 629 (1994)

[33] M. Hilgendorff, V. Sundström, J. Phys. Chem. B 102, 10505 (1998)

[34] G. Ramakrishna, H. N. Ghosh, J. Phys. Chem. B 105, 7000 (2001)

[35] D. El Mekkawi, M. S. A. Abdel-Mottaleb, Int. J. Photoenergy 7, 95 (2005)

Table 1. Photoelectric conversion properties of WE-N, WE-N-BA, WE-N-s, and WE-N-s-BA.

Electrode	I_{SC} / μA cm^{-2}	V_{OC} / V	*FF*	P_{max} / μW cm^{-2}
WE-N	14.1	0.20	0.33	0.94
WE-N-BA	13.8	0.21	0.35	1.0
WE-N-s	19.1	0.43	0.37	3.0
WE-N-s-BA	22.0	0.43	0.38	3.6

I_{SC} : short circuit photocurrent density

V_{OC} : open circuit voltage

FF : fill factor

P_{max} : maximum power

Figure captions

Figure 1 SEM images of (a) the steam-treated titania electrodes, WE-N-s, and (b) the steam-treated benzoic acid-doped titania electrode, WE-N-s-BA

Figure 2 XRD patterns of the untreated and steam-treated titania films, F-N and F-N-s, and the untreated and steam-treated benzoic acid-doped titania films, F-N-BA and F-N-s-BA, respectively

Figure 3 $I-V$ curves of the untreated and steam-treated titania electrodes, WE-N and WE-N-s, and the untreated and steam-treated benzoic acid-doped titania electrodes, WE-N-BA and WE-N-s-BA, respectively, during UV irradiation

Figure 4 Time course of the concentrations of (1) CO_2 and (2) H_2O in the gas phase during the photocatalytic degradation of benzoic acid for the steam-treated benzoic acid -doped titania electrodes, WE-N-s-BA

Figure 5 FTIR spectra of the steam-treated benzoic acid-doped titania electrode, WE-N-BA, (1) before and after (2) 1-h and (3) 3-h UV irradiations

Figure 1

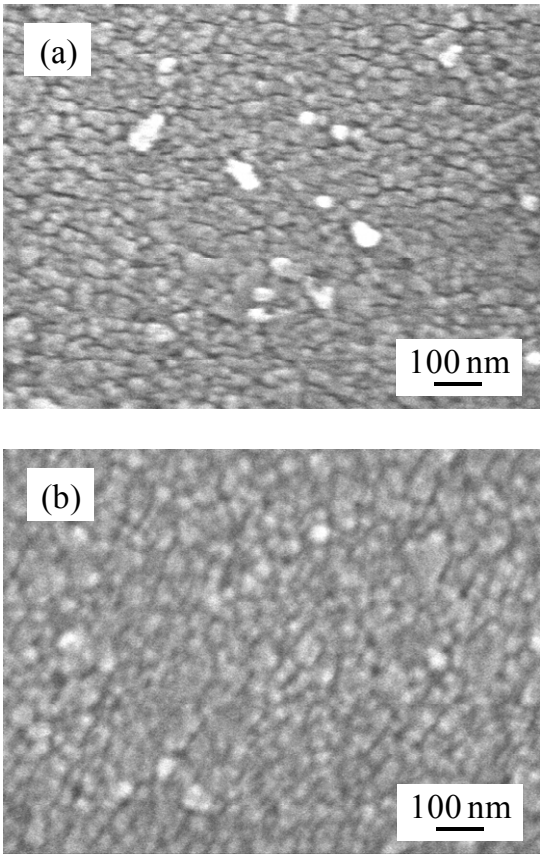

Figure 2

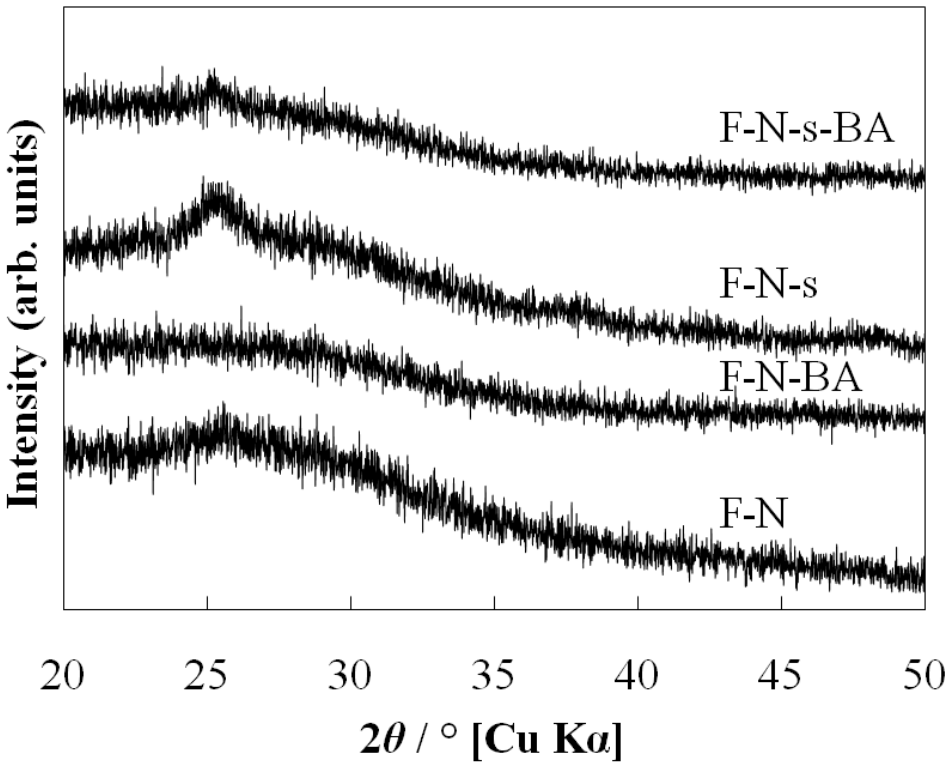
Intensity (arb. units)
F-N-s-BA
F-N-s
F-N-BA
F-N
20
25
30
35
40
45
50
2θ / ° [Cu Kα]

Figure 3

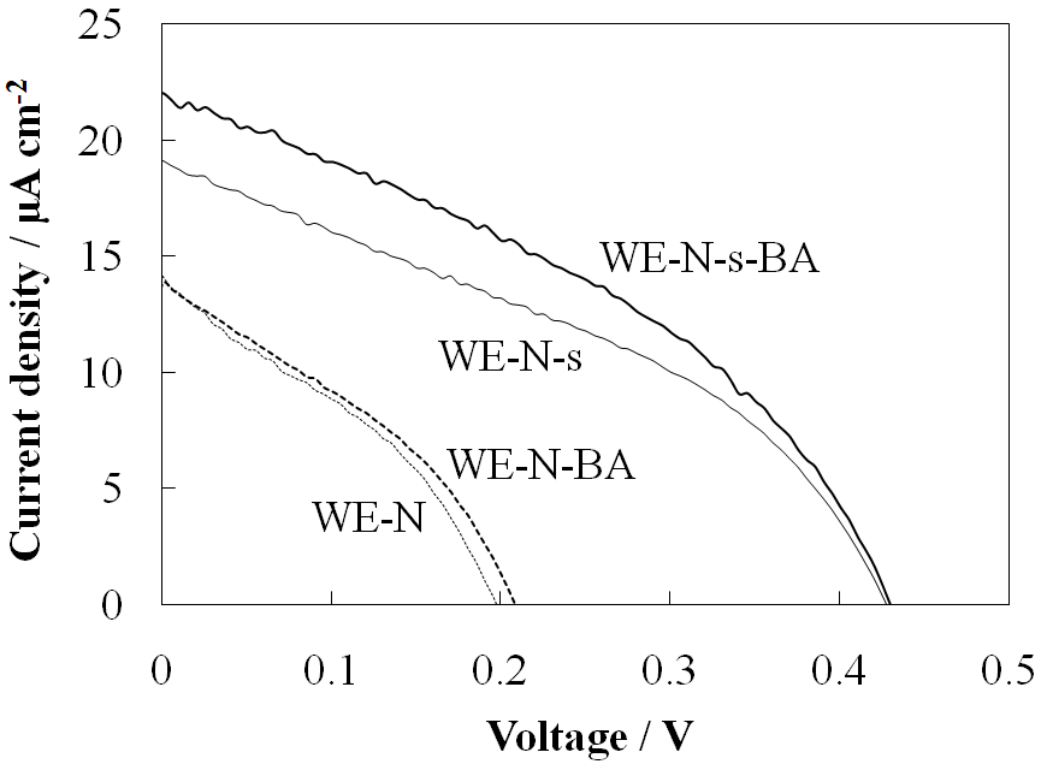
Current density / μA cm-2
25
20
15
10
5
0
0
0.1
0.2
0.3
0.4
0.5
Voltage / V
WE-N-s-BA
WE-N-s
WE-N-BA
WE-N

Figure 4

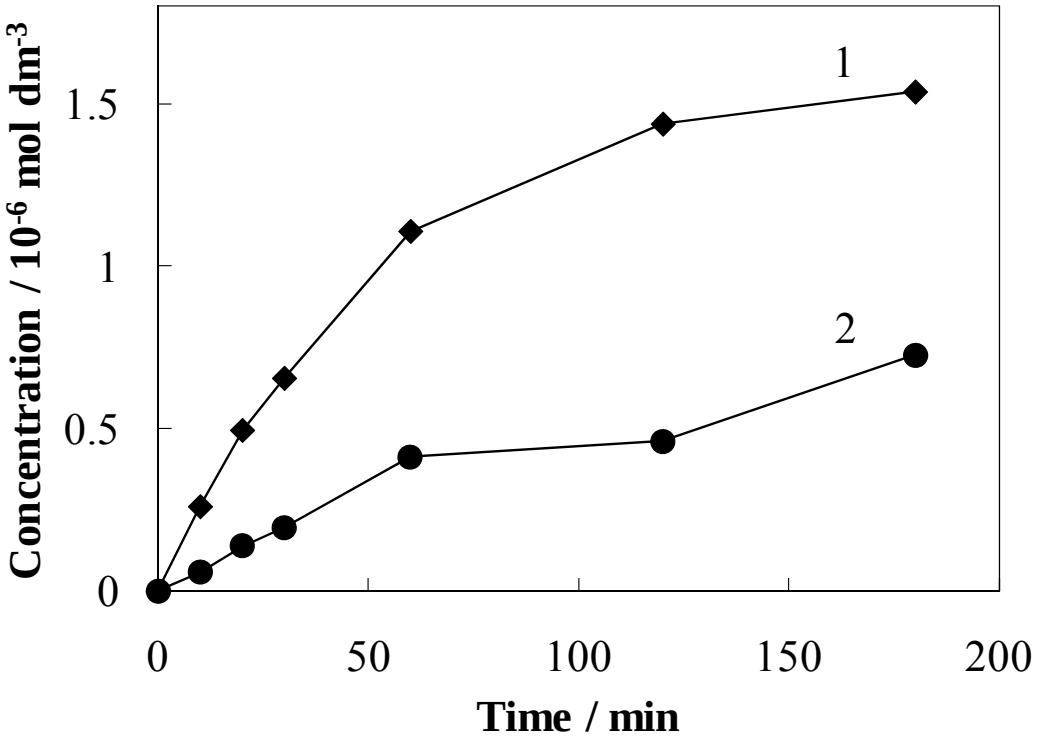

Figure 5

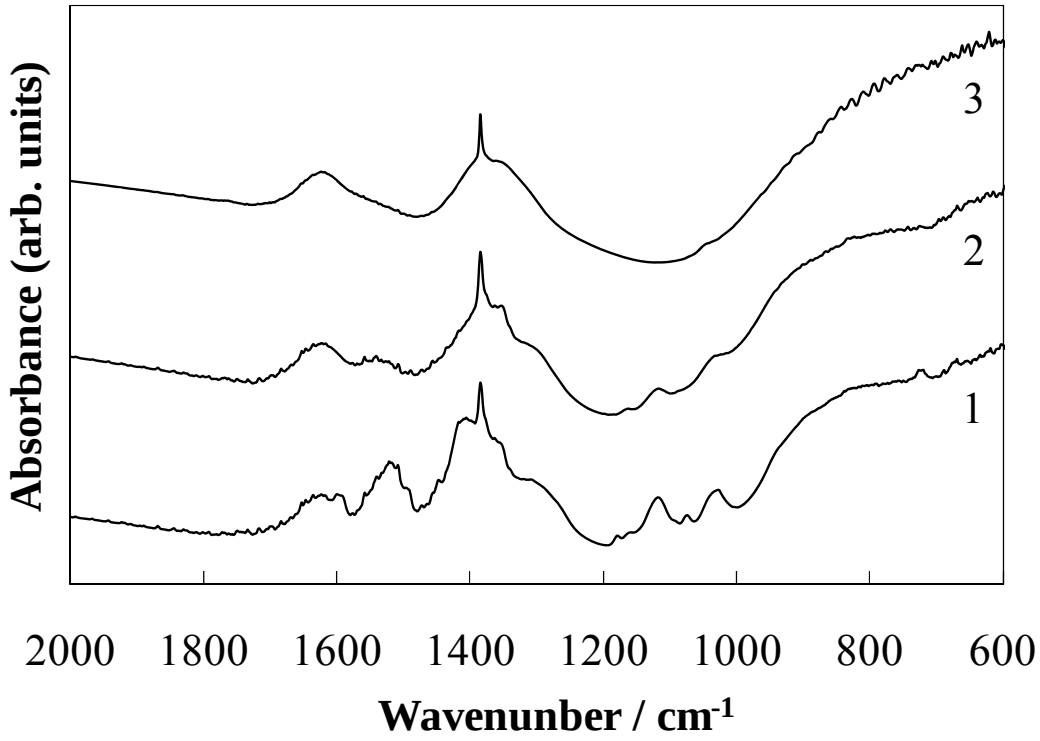
Absorbance (arb. units)
3
2
1
2000
1800
1600
1400
1200
1000
800
600
Wavenunber / cm-1